Eur. Phys. J. D **10**, 259–263 (2000)

THE EUROPEAN PHYSICAL JOURNAL D

EDP Sciences

Magnetisation of isolated single crystalline Fe-nanoparticles measured by a ballistic Hall micro-magnetometer

L. Theil Kuhn[1,a], A.K. Geim[2], J.G.S. Lok[2], P. Hedegård[1], K. Ylänen[1], J.B. Jensen[1], E. Johnson[1], and P.E. Lindelof[1]

[1] Ørsted Laboratory, Niels Bohr Institute, Universitetsparken 5, 2100 Copenhagen Ø, Denmark
[2] Research Institute for Materials, University of Nijmegen, 6525 Nijmegen, The Netherlands

Received: 1st September 1998 and Received in final form 21 June 1999

Abstract. We present here the first magnetisation measurements on isolated single crystalline Fe-nanoparticles performed with a ballistic Hall micro-magnetometer. The measurements have a sensitivity of $10^4 \mu_B$ and thus provide us the possibility to study the mechanisms of magnetisation reversal in a single nanoparticle. The magnetic properties of the nanoparticles are influenced by their crystal structure and shape, and the presence of an oxide surface layer. They exhibit curling of the magnetic moments, but also a novel hysteresis behaviour. The spin configurations found for the system agree well with numerical calculations based on a Heisenberg Hamiltonian including the exchange and dipole interaction and surface anisotropy.

PACS. 07.55.Jg Magnetometers for susceptibility, magnetic moment, and magnetization measurements – 36.40.Cg Electronic and magnetic properties of clusters – 61.46.+w Clusters, nanoparticles, and nanocrystalline materials

1 Introduction

There exists a wide range of magnetisation and flux pinning measurements on lithographically produced nanostructures performed with magnetometers based on the classical Hall effect in the diffusive transport regime of a two-dimensional electron gas [1–3]. In contrast to such investigations we have used Hall micro-magnetometers based on ballistic electron transport for studying the flux penetration and the magnetisation of single lithographically produced disks (diameters 1.0 μm−0.1 μm) of either superconducting or magnetic materials [4,5] or nanoparticles.

Here we present the first magnetisation measurements on isolated single crystalline Fe-nanoparticles in the size range 5 nm to 50 nm. This gives us the opportunity to study the mechanisms of domain formation and the reversible and irreversible parts of the magnetisation dynamics. Particularly the fact that the nanoparticles have a build-in symmetric crystal field and are perfectly faceted crystals as well as the presence of a well-defined oxide surface layer allow us to gain insight in the problem of anisotropy and the magnetic core-shell system.

[a] *Present address*: Laboratory of Solid State Physics and Magnetism, Katholieke Universiteit Leuven, Celestijnenlaan 200D, 3001 Leuven, Belgium.
e-mail: `theil@fys.ku.dk`

2 Samples

The samples consist of a series of five ballistic Hall micro-magnetometers. On four of them a single magnetic nanoparticle is deposited, while the fifth is used as a local sensor of the applied magnetic field. The magnetometers are fabricated from a two-dimensional electron gas (2DEG) embedded in a GaAs–GaAlAs heterostructure and defined by means of electron beam lithography. The sensitive area of each device is less than 1×1 μm^2 and the distance from the surface to the 2DEG is 60 nm.

2.1 Hall micro-magnetometer

The classical Hall magnetometer is based on the principle that the linear Hall resistance of a 2DEG arising from an applied magnetic field is known and therefore an unknown magnetic flux can be studied. In general, the Hall resistance R_{Hall} of a 2DEG is proportional to the magnetic flux density B, the electron sheet density n, and the electronic charge e in the following way $R_{\mathrm{Hall}} \propto B/ne$.

To be able to study the details of the magnetisation of a single ferromagnetic nanoparticle with less than 10^6 Bohr magnetons (μ_B), the sensitivity of the Hall magnetometer must be several orders of magnitude better than in the above mentioned experiments [1–3], which all were done using Hall magnetometers based on diffusive electron transport, which measures the *average* magnetic flux

in the Hall magnetometer area. As described in [6] ballistic electron transport probes *locally* the magnetic flux in the Hall device, since the electrons are not scattered before detection in the voltage leads. It thus provides much more detailed information about the *local* magnetic flux distribution.

Ballistic electron transport suffers from several complications in the form of non-linear effects like the negative Hall effect or the complete quenching of it [7,8]. To ensure that the magnetisation measurements were performed in the linear regime, the mobility and the electron density in the Hall micro-magnetometer is chosen such that the electron transport is just ballistic, meaning a not too long mean free path as compared to the dimensions of the Hall device. For the devices used the mobility at low temperatures is 30 m^2/Vs and the effective electron density is 2×10^{15} m^{-2} resulting in a mean free path of 2.6 μm. At liquid helium temperatures various quantum effects in the 2DEG set in and the linear Hall resistance is disturbed by universal conductance fluctuations. A method to prevent this is simply to apply a relatively large current of several μA. The magnetic field on the surface of the magnetometer produced by this current is an order of magnitude smaller than the sensitivity of the magnetometer, it does therefore not alter the magnetisation measurements.

The geometry of the Hall device is also important: if the corners are too rounded the electrons are multiply reflected and a suppression or a quench of the Hall effect is more pronounced.

2.2 Nanoparticles

The Fe-nanoparticles are fabricated in a hollow cathode cluster source [9] from condensation of a super-saturated metal vapour, and they are during formation covered with a thin layer of protective oxide.

To characterise the single nanoparticles they have been studied with both scanning electron microscopy (SEM), atomic force microscopy (AFM), transmission electron microscopy (TEM), electron micro-diffraction, and X-ray diffraction. The Fe-nanoparticles are 5 nm to 50 nm from facet to facet with a peak in the size distribution at 15 nm. The TEM images in Figure 1 show that they are single crystals with the shape of truncated cubes. The single crystalline cubes have the bcc structure of α-Fe with a lattice constant of $a = 2.90 \pm 0.03$ Å.

A thin layer of oxide covers the Fe-nanoparticles (in Fig. 1b) visible as a light grey shell) formed naturally on the particle's surface due to residual oxygen in the cluster source. This oxide is very stable on the time scale of weeks and protects the nanoparticle against further oxidation when the samples are transferred from the cluster source to the various characterisation experiments. The oxide layer on the Fe-nanoparticles consists mainly of γ-Fe_2O_3, but also Fe_3O_4 is formed in very small amounts. It has a thickness of 2.0 nm to 2.5 nm independent of the nanoparticle size [10]. These findings are consistent with previous studies of slowly formed oxide on Fe-nanoparticles [11].

The Hall micro-magnetometers are mounted perpendicular to the beam of clusters and the nanoparticles are soft-landed on the surface, so neither the magnetometers nor the nanoparticles are damaged.

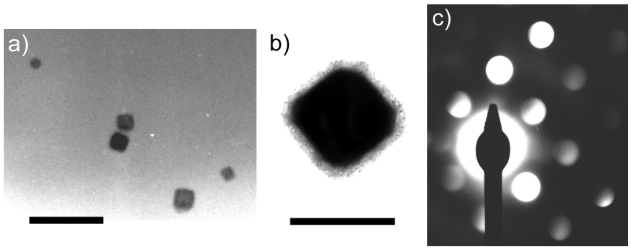

Fig. 1. Transmission electron micrographs of Fe-nanoparticles deposited on amorphous Carbon-film; (a) shows an overview of several deposited Fe-nanoparticles, the black bar is 100 nm; (b) shows a zoom on a single faceted 15 nm Fe-nanoparticle with a thin oxide layer on the surface (the light grey shell). The electron beam axis is (001). The black bar is 15 nm; (c) shows the electron micro-diffraction pattern from the single Fe-nanoparticle shown in (b). From analysis of the diffraction spots the particle clearly has the bcc crystal structure of α-Fe with a lattice constant $a = 2.90 \pm 0.03$ Å.

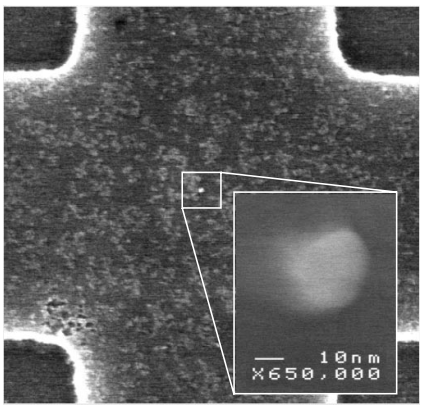

Fig. 2. SEM picture of a 1×1 μm^2 Hall micro-magnetometer with a single Fe-nanoparticle (white dot) placed in the sensitive centre region. The magnification (white frame) shows that the Fe-nanoparticle is 20 nm.

2.3 Single nanoparticle selection

To select a few or a single nanoparticle we prepare the Hall micro-magnetometers with a layer of PMMA on the surface with a 100 nm opening made using electron beam exposure and development at the centre region of the magnetometer. The nanoparticles are deposited and subsequently the PMMA with the excess nanoparticles is removed, and only a few nanoparticles are left on the micro-magnetometer.

The surface is scanned with an AFM in the vibrating cantilever mode and the nanoparticles are located. Only one nanoparticle is positioned in the centre of the sensitive area of each of the magnetometers. The rest of the nanoparticles is removed by AFM manipulation as described in [12].

Figure 2 shows a SEM picture of a 1×1 μm^2 Hall micro-magnetometer with a single 20 nm Fe-nanoparticle

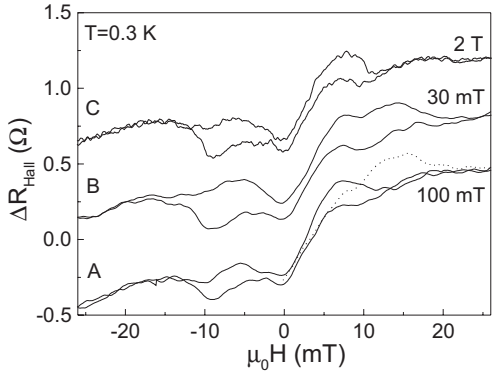

Fig. 3. A set of hysteresis loops for the 20 nm Fe-nanoparticle shown in Figure 2, the loops B and C are offset for clarity. The linear background Hall resistance has been subtracted. The net magnetisation of the nanoparticle is directly proportional to ΔR_{Hall} by the factor 2.7×10^{-7} $\Omega/(\mathrm{A/m})$. Discussion in text.

placed in the centre, the inset shows a magnification of the nanoparticle. The resolution of this SEM picture can not compete with the TEM images in Figure 1, and the cubic shape of the nanoparticle is therefore not visible here. In another experiment, where the AFM and SEM studies were devoted to the imaging of the Fe-nanoparticles on GaAs, we found that the Fe-nanoparticles keep their cubic shape after they have been deposited on the GaAs.

3 Magnetisation measurements

After placing a single ferromagnetic nanoparticle in the sensitive region of the Hall micro-magnetometer it is cooled to liquid helium temperatures, and the Hall resistance is measured using standard four-terminal AC-lockin technique. The hysteresis loops presented here have been obtained after subtraction of the linear background Hall resistance, caused by the homogeneous applied magnetic field, from the measured Hall resistance. The additional Hall resistance ΔR_{Hall} is caused by the induced magnetic field from the nanoparticle. ΔR_{Hall} has been proved to be linearly related to the magnetisation of the nanoparticle [6]. For more details on the measuring technique we refer to [4–6].

3.1 Magnetisation of a single nanoparticle

Figure 3 shows a set of hysteresis loops measured on the isolated cubic 20 nm Fe-nanoparticle shown in Figure 2. The linear background Hall voltage has been subtracted. The measurements were performed after zero-field cool down to 0.3 K.

Several novel features are present: the hysteresis loop A starts with the virgin trace (dotted line) at a small negative value changing to a positive value as the external magnetic field is increased. The field is swept to 100 mT and then reduced and reversed towards −100 mT. It is remarkable that the hysteresis loop does not exactly follow the virgin trace. The virgin traces for the loops B and C have been omitted in Figure 3 since they are identical to that of A.

Loop B shows the hysteresis loop when the magnetic field is reversed at ±30 mT. The shape of the hysteresis loop B resembles partly the virgin trace (as shown for A) and loop A, but loop B is more open than A. Loop C is the hysteresis loop recorded during a magnetic field sweep of ±2 T. This loop resembles loop A.

At an applied magnetic field of 15 mT the loops A and C appear magnetically saturated, while loop B appear saturated at 26 mT. All the hysteresis loops exhibit coercive fields of approximately 2 mT, and they are not symmetric for opposite applied magnetic fields.

The areas of the hysteresis loops depend on the maximum applied magnetic fields up to approximately 100 mT, although the hysteresis loops appear to have reached saturation at much lower fields.

4 Discussion

From the hysteresis loops in Figure 3 it is evident that the 20 nm Fe-nanoparticle is ferromagnetic. Apparently saturation is reached for an applied field below the characteristic saturating field of 50 mT for a perfect single domain Fe-crystal [14]. There are no Barkhausen jumps on the hysteresis loops signalling movements of domain walls as we have observed earlier for multi domain Ni-disks [4,5].

The hysteresis loops exhibit small coercive fields much smaller than the saturating fields, so the magnetisation reversal of the Fe-nanoparticle does not take place by a coherent turning of the spins like in a perfect single domain nanoparticle. The detailed structure of the hysteresis loops also indicates that the magnetisation reversal is not well described by the simple Néel-Brown model of thermal switching of the magnetisation over one anisotropy barrier between two opposite states nor by the Stoner-Wohlfarth model of coherent reversal [15–17].

We suggest that, since the 20 nm Fe-nanoparticle is approximately the size of a Bloch wall [16], and since it has the cubic shape, it is energetically favourable for the spins to arrange themselves in a vortex structure. The vortex would for a larger cubic particle evolve into four 90 degree domains. When applying a magnetic field the spins are gradually turned out of the vortex structure through the incoherent curling mode [16]. The hysteresis loop becomes smooth, because the magnetisation process involves only the turning of individual spins. The saturating field is connected to the anisotropy hindering the spin reversals rather than the Bloch wall energy.

Vortex formation implies a zero net magnetic moment of the Fe-nanoparticle at zero applied magnetic field, a saturating magnetic field weaker than that of a single domain nanoparticle, and a small coercive field [16]. The detailed structure of the hysteresis loops is caused by the curling type of incoherent turning of the spins during magnetisation reversal. The easy magnetisation axes in combination with the surface of the cubic Fe-nanoparticle can make some spin configurations more stable than others,

and more configurations almost similar in energy might exist. Therefore the magnetisation reversal is not a continuous process and bumps appear, just like a curling version of Barkhausen jumps in a multi domain particle. The bumps in the hysteresis loop can be caused by intermediate locking of the spins to the easy axes of the Fe-cube (for α-Fe equal to the crystal axes), since the orientation of the Fe-nanoparticle during the magnetisation reversal is fixed relative to the surface of the magnetometer. The presence of several spin configurations of similar energy produces an asymmetric hysteresis loop around $\mu_0 H = 0$ and possibly also the "overshooting" of the virgin trace. In the references [5,13,17] the incoherent curling type of magnetisation reversal in nanoparticles was also observed.

4.1 Numerical model for the spin configurations

To justify our suggestion of a vortex-like structure and a curling type behaviour during magnetisation reversal, we simulated the spin system by a simple numerical model. We chose a Heisenberg Hamiltonian with 512 spins distributed on a cubic grid with nearest neighbour exchange interaction, dipole interaction and surface anisotropy. Shape anisotropy is indirectly included via the missing neighbouring spins at the surface. The surface breaks the cubic symmetry, and it introduces an exchange anisotropy. The surface anisotropy has been included as a phenomenological constant favouring spins oriented parallel to the surface, since this results in the lowest energy.

The Hamiltonian is minimised by use of Lagrange multipliers. The minimisation is done by starting with a guess of a configuration and then finding local minima by iteration from that one. The number of spins can be increased to resemble the number in the 20 nm Fe-nanoparticle by the use of scaling factors on the interaction energies in the calculation.

The energetically most favourable zero-field spin configuration turns out to be strongly dependent on the size and the surface anisotropy. For a cubic Fe-nanoparticle with a surface anisotropy equal to what has been experimentally found for almost spherical Fe-nanoparticles with low surface anisotropy $K_\mathrm{s} = 10^{-4}$ J/m^2 [18], the simulation showed that the cross-over from a ferromagnetic single domain to a vortex-like arrangement of the spins happens at approximately a size of 20 nm. By increasing the surface anisotropy the vortex configuration is favoured also at smaller sizes. The shape and surface anisotropy causes the vortex to deviate from a perfectly circular vortex, so it has a small net magnetisation out of the plane of the vortex.

We added an external magnetic field to the Hamiltonian as a Zeeman term and simulated the magnetisation process. We observed that from the vortex configuration the spins turned incoherently following the curling mode and the major part of them were aligned at an external field of 4 mT (for $K_\mathrm{s} = 10^{-4}$ J/m^2). However, a minority of the spins were very hard to align, even at 100 mT the cube was not fully magnetically saturated. Above 2 T a full ferromagnetic alignment was achieved.

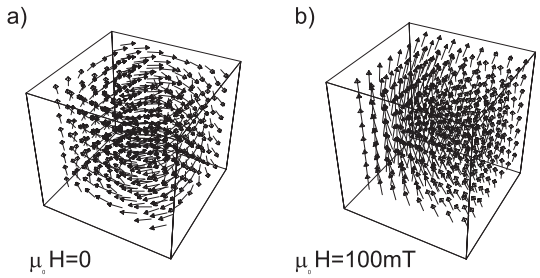

Fig. 4. Simulation of the spin configurations for a 20 nm cubic Fe-nanoparticle with $K_\mathrm{s} = 10^{-4}$ J/m^2: (a) for zero external magnetic field and (b) an almost saturating magnetic field.

Figure 4 shows the vortex and the curling configurations. We observed that on the path of the magnetisation-demagnetisation cycle many metastable spin configurations exist. They depend critically on the proceeding configuration, so the hysteresis loop exhibits structure and is non-symmetric for opposite directions of the external field. This behaviour, which was also observed in [17], and the values of the coercive field (4 mT) and the apparently saturating field (100 mT) resembles well our magnetisation measurements as presented in Figure 3.

4.2 Influence of the oxide surface layer

The 2 nm γ-Fe_2O_3/Fe_3O_4 surface layer on the Fe-nanoparticle is ferromagnetically ordered [19]. This introduces an additional magnetic anisotropy in the nanoparticle. The spins in the γ-Fe_2O_3/Fe_3O_4 are placed in crystallites of maximum size 2 nm. Such small crystallites of γ-Fe_2O_3/-Fe_3O_4 are known to exhibit ferromagnetism due to canting of the spins [18], and they are therefore very hard to align. This can explain the apparent saturation in the hysteresis loops A, B, and C. Loop B shows that 30 mT only saturates the main part of the spins in the Fe core, while the canted γ-Fe_2O_3/Fe_3O_4 surface layer remains unsaturated. Loops A and C show that above 100 mT no changes appear, so both the Fe core and the γ-Fe_2O_3/Fe_3O_4 surface layer are magnetically aligned. The magnetic coupling between the ferromagnetic Fe and the canted ferromagnetic γ-Fe_2O_3/Fe_3O_4 influences the spin configurations during magnetisation reversal and causes the hysteresis loop to not follow the virgin trace and to be non-symmetric, so the nanoparticle exhibit a memory effect [5]. The surface anisotropy constant in the simulation represents this magnetic anisotropy. Furthermore, the magnetic coupling between the core and the shell possibly causes the slight shift of the hysteresis loops. This is observed in layered systems with an oscillatory behaviour of the exchange constant, and here it might be caused by the difference in exchange interaction over the interface [16].

5 Conclusion

We have here studied the magnetisation of an individual 20 nm Fe-nanoparticle by a ballistic Hall micromagnetometer of sensitivity $10^4 \mu_\mathrm{B}$. It proved to be a good

alternative to the SQUID [13], since it can be used with a comparable sensitivity in a much broader temperature range ($T < 80$ K) and in magnetic fields up to several tesla applied in any direction. Most importantly, it does not interact magnetically with the object studied. It will be possible in the future to improve the sensitivity of the ballistic Hall micro-magnetometer by reducing the detection area further and by moving the 2DEG to the surface.

We found that the most probable spin configuration for the cubic single crystalline 20 nm Fe-nanoparticle is a vortex structure, which during magnetisation reversal exhibits curling. The canted γ-Fe_2O_3/Fe_3O_4 surface layer introduces an additional anisotropy by magnetic coupling. We propose that there exist several different spin configurations during the magnetisation reversal process, which gives rise to a very detailed hysteresis loop and a memory effect.

We are very grateful to S.V. Dubonos from the Institute of Microelectronics in Chernogolovka for having provided the first Hall micro-magnetometers. This project was financially supported by the Danish Research Council, CNAST, the Velux Foundation and the European Commission's TMR-Programme.

References

1. S. Wirth, M. Field, D.D. Awschalom, S. von Molnár, Phys. Rev. B **57**, R14028 (1998).
2. A.D. Kent, S. von Molnár, S. Gider, D.D. Awschalom, J. Appl. Phys. **76**, 6656 (1994).
3. E. Shung, T.F. Rosenbaum, M. Sigrist, Phys. Rev. Lett. **80**, 1078 (1998).
4. A.K. Geim, S.V. Dubonos, J.G.S. Lok, I.V. Grigorieva, J.C. Maan, L. Theil Hansen, P.E. Lindelof, Appl. Phys. Lett. **71**, 2379 (1997).
5. J.G.S. Lok, A.K. Geim, J.C. Maan, S.V. Dubonos, L. Theil Kuhn, P.E. Lindelof, Phys. Rev. B **58**, 12201 (1998).
6. F.M. Peeters, X.Q. Li, Appl. Phys. Lett. **72**, 572 (1998).
7. C.W. Beenakker, H. van Houten, Phys. Rev. Lett. **63**, 1857 (1989).
8. C.J.B. Ford, T.J. Thornton, R. Newbury, M. Pepper, H. Ahmed, D.C. Peacock, D.A. Ritchie, J.E.F. Frost, G.A.C. Jones, Phys. Rev. B **38**, 8518 (1988).
9. L. Theil Kuhn, Ph.D. thesis, Niels Bohr Institute, University of Copenhagen, 1999.
10. K.N. Clausen, F. Bødker, M.F. Hansen, L. Theil Kuhn, K. Lefmann, P.A. Lindgård, S. Mørup, M. Telling, Physica B (to appear, 2000).
11. S. Linderoth, S. Mørup, M.D. Bentzon, J. Mat. Sci. **30**, 3142 (1995).
12. L. Theil Hansen, A. Kühle, A.H. Sørensen, J. Bohr, P.E. Lindelof, Nanotechnology **9**, 337 (1998).
13. W. Wernsdorfer, E. Bonot Orozco, K. Hasselbach, A. Benoit, B. Barbara, N. Demoncy, A. Loiseau, H. Pascard, D. Mailly, Phys. Rev. Lett. **78**, 1791 (1997).
14. C. Kittel, *Introduction to Solid State Physics* (Wiley, New York, 1996).
15. W.F. Brown Jr, Phys. Rev. **130**, 1677 (1963).
16. B.D. Cullity, *Introduction to Magnetic Materials* (Addison-Wesley, Reading, 1972).
17. M. Lederman, S. Schultz, M. Osaki, Phys. Rev. Lett. **73**, 1986 (1994).
18. F. Bødker, S. Mørup, S. Linderoth, Phys. Rev. Lett. **72**, 282 (1994).
19. Recently found by X-ray magnetic circular dichroism performed by K. Fauth, E. Goering, L. Theil Kuhn at ESRF, the analysis will be published elsewhere.